THE ASTROPHYSICAL JOURNAL, 347:52–58, 1989 December 1

SUPERCLUSTERING OF QUASI-STELLAR OBJECT ABSORPTION CLOUDS

JULIA HEISLER, CRAIG J. HOGAN, AND SIMON D. M. WHITE
Steward Observatory, University of Arizona
Received 1989 March 6; accepted 1989 May 31

ABSTRACT

We examine the clustering of C IV absorption line systems along the lines of sight to the 55 quasars in the survey of Sargent, Boksenberg, and Steidel. We confirm their original result that there is strong clustering of these systems at separations less than 1000 km s^{-1}. We show that the peculiar velocities of the clouds combine with the one-dimensional nature of the sampling to preclude any detailed comparison of the observed clustering strength on these scales with that found for nearby systems such as galaxies. We show that the sample also contains significant clustering on larger scales, 1000–10,000 km s^{-1}. This probably reflects true spatial clustering of an amplitude exceeding that observed for any nearby systems, even rich clusters of galaxies. The signal is due mainly to high equivalent width absorbers and is dominated by a single very large "absorption supercluster" in the quasar 0237−233. It seems likely that this structure was produced by processes other than gravitational instability.

Subject headings: cosmology — galaxies: clustering — quasars

I. INTRODUCTION

The spectra of QSOs display numerous absorption features, many of which result from foreground clouds of gas unrelated to the quasar. The line systems which show absorption due to heavy elements (i.e., C, N, O, or S) in addition to hydrogen are thought to arise in gaseous coronae around galaxies or protogalaxies. The distribution of these systems with redshift thus contains information about the cosmological evolution of such objects, their clustering and their motions. The simplest statistic containing information about the latter two questions is probably the autocorrelation of the systems in redshift space. At small velocity lags this statistic is heavily influenced by the peculiar velocities of the clouds in their local environment, while at larger lag it is expected to reflect their large-scale clustering. Both kinds of information are useful for studying the formation and distribution of galaxies at early epochs. They complement information from the variation with redshift of the overall abundance, excitation, and metallicity of the clouds.

Studies of these systems have recently been greatly facilitated by complete and homogeneous surveys of the spectra of large numbers of QSOs. In this paper we study the autocorrelation function of heavy element absorbers in the high-resolution, high signal-to-noise survey of Sargent, Boksenberg, and Steidel (1989; hereafter SBS). These authors estimated the small-scale clustering in their data, and noted some evidence for large-scale clustering. With some revision of their quantitative results, we confirm their basic conclusions. Our analysis demonstrates the startling result that the autocorrelation function for their data set is nonzero out to 10,000 km s^{-1} at the $\sim 4\ \sigma$ significance level. The implied clustering amplitude is much larger than that observed for galaxies at low redshift, and is larger even than that claimed for rich clusters of galaxies (Bahcall and Soneira 1983; Klypin and Kopylov 1983; but see Sutherland 1988; Dekel *et al.* 1989). Closer examination of the sample shows that most of this clustering signal comes from high equivalent width systems in a single, very large "absorption supercluster." In § II below we discuss the meaning of the redshift-space correlation function, and in § III the techniques we use to estimate it. Section V then presents results for the SBS data set. A concluding section discusses the implications of these results for the nature and large-scale distribution of the absorbing clouds.

II. REDSHIFT-SPACE CORRELATION FUNCTIONS

The relationship between the three-dimensional spatial autocorrelation of absorbers, $\xi(r)$, and the observable line of sight, or redshift-space correlation, $\xi_v(v)$, is straightforward. At velocity differences much smaller than c we may neglect geometric effects and write the simple convolution,

$$\xi_v(v) = \int_0^\infty H\, dr\, \xi(r) P(v \mid r)\ . \tag{1}$$

The function, $P(v \mid r)dv$, is the probability of seeing a velocity difference in the range $(v, v + dv)$ for a pair with true line-of-sight separation, r. If the absorbing clouds were at rest with respect to the comoving frame, then we would have $P = \delta(v - Hr)$, leading to $\xi_v(v) = \xi(v/H)$. In fact, of course, the peculiar velocities of the clouds will not be zero. It is instructive to study the properties of this relationship using the simple model, $\xi(r) = (r/r_0)^{-\gamma}$, which fits clustering data for nearby galaxies, together with the assumption that the relative peculiar velocity of pairs has a Gaussian distribution independent of r. Equation (1) then becomes

$$\xi_v(v) = (2\pi)^{-1/2} \int_0^\infty \frac{H\, dr}{\sigma} \left(\frac{r}{r_0}\right)^{-\gamma} \times \left\{ \exp\left[-\frac{(Hr - v)^2}{2\sigma^2} \right] + \exp\left[-\frac{(Hr + v)^2}{2\sigma^2} \right] \right\}\ , \tag{2}$$

where there are two exponential terms because we are defining both r and v to be positive.

The first important thing to note about equation (2) is that it diverges at its lower limit. This problem is artificial in that a more careful derivation shows this simple form to be valid only on scales larger than the physical size of the absorbers. With an appropriate modification the integral converges rapidly on smaller scales, so one can approximately take the lower limit to be the cloud radius, r_{cl}. However, the amplitude of ξ_v at small velocity separations then becomes proportional to $(r_{cl}/r_0)^{-\gamma}$. Since r_{cl} is very poorly known, the small-scale clustering strength of the absorbers cannot be meaningfully compared with that derived from three-dimensional surveys for other classes of object (e.g., galaxies). In addition, specific detailed models (e.g., Salmon and Hogan 1986) show that for $Hr \lesssim \sigma$, $(v - Hr)$ and r are not actually independent. On the other hand, for $Hr \gg \sigma$ both of these problems disappear: we recover $\xi_v(v) \approx \xi(v/H)$, and the spatial clustering of the systems is estimated directly. The shape predicted for ξ_v for this model is thus a Gaussian of width σ and height determined by r_{cl} joining smoothly onto a power-law tail which is just $\xi(v/H)$. Although our model for the peculiar velocity distribution is too simple to be correct, it should be adequate to give the main features of ξ_v. Based on observations of nearby galaxies and clusters one might guess that $\sigma \sim 300$ km s^{-1} (Davis and Peebles 1983). It seems safe to use ξ_v to derive $\xi(r)$ only at separations exceeding 1000 km s^{-1}. Interpretation of the data at smaller velocity lags requires knowledge both of the structure and of the detailed kinematics of the absorbing clouds.

III. ESTIMATES OF ξ_v

Our major task is to estimate ξ_v as reliably as possible for the 229 C IV absorption systems found in the spectra of 55 quasars by SBS. This compilation includes the equivalent width of each C IV absorption, as well as the redshift range within each spectrum over which such absorption systems could have been found and for which identifications are complete. The sample contains absorbers with redshifts ranging from 1.27 to 3.53 with median $z = 1.87$. It is designed to contain all systems with equivalent width in each member of the C IV doublet exceeding 0.15 Å; in fact, about half of the systems in the sample satisfy this criterion. For some of our analysis we will restrict ourselves to subsamples split according to the equivalent width or redshift range of the absorbers. Both the abundance of absorbing clouds and their clustering properties undoubtedly evolve over the redshift range spanned by this sample. We design our estimator for ξ_v to be independent of the evolution of cloud abundance and to be optimal when ξ_v is independent of redshift. The latter assumption is arbitrary; we could just as easily have assumed clustering to be constant as a function of comoving separation. We shall see that there is not enough data in the present sample to distinguish these possibilities. Our assumption has the advantage that the resulting estimates are independent of cosmological model; they can be interpreted as an appropriately weighted average of the clustering strength over the redshift range of the sample.

A detailed description of our estimate of ξ_v follows:

1. We decide on a set of bins in v for each of which we intend to estimate ξ_v. The following steps are then followed to estimate ξ_v in each bin.[1]

2. For each absorption system in each QSO, we determine the range of redshifts whose velocity separations from the system lie within the current bin and for which C IV systems could have been detected. This range can consist of 0, 1, or 2 redshift intervals, each of which may be narrower than the original velocity bin.

[1] Bin boundaries in v were determined by requiring approximately equal numbers of expected random pairs in each bin once statistics were accumulated for the sample as a whole. This results in equal sensitivity to departures from an unclustered distribution in each bin. The resulting bins get broader at larger v.

3. We then augment the count of observed pairs within the current bin by the number of C IV systems found in the various redshift intervals. In addition, we augment the number of random pairs expected in the bin by an estimate computed as follows.

4. We estimate a random density of absorbers at the position of each redshift interval by dividing the number of absorption systems within $\pm 25{,}000$ km s^{-1} of its center in the 54 *other* QSOs by the total pathlength in this redshift range for which C IV lines could have been detected in them. We then multiply this density by the length of the redshift interval under consideration to estimate the expected number of random systems it should contain. This technique automatically takes out any variation in cloud abundance with redshift without need for model fitting. In addition it ensures that the counting noise in the estimate of the number of random pairs is much smaller than that in the number of observed pairs.

5. Finally we obtain an estimate of $1 + \xi_v(v)$ by dividing the total number of observed pairs in each bin by the total number of expected pairs. This should be an efficient estimator of ξ_v because each observed pair is given equal weight. In the absence of clustering this estimate is expected to scatter around unity with variance equal to the inverse of the expected number of pairs (each counted once). This allows us to plot an error estimate. However, for a clustered distribution the uncertainty will be larger than this, even on scales much larger than that of the clustering, because pairs are no longer independent of each other.

The above scheme is quite complex and was arrived at after considerable experimentation with Monte Carlo data sets. We set up such artificial data by using a Poisson random number generator to put down systems at random over the accessible redshift range in each of the 55 QSOs. We could then use the same analysis program as on the real data to check that our estimate of ξ_v is unbiased, and does indeed scatter about zero as expected from the above argument. We made artificial data sets in which the density of systems depended on redshift to check that our estimate is indeed unaffected by any such dependence. We also tried putting down systems in pairs of relatively small separation to verify that the rms scatter in our ξ_v estimate at large v is then increased by a factor of 2. Figure 1 is a diagrammatic explanation of our estimating procedure which may help clarify the above discussion.

IV. RESULTS

Our estimates of the redshift-space correlation are shown in Figures 2–5 for various subsamples of the SBS data set. Figure 2 shows results when lines of all equivalent widths are used, while Figure 3 shows corresponding estimates for the 98 systems with equivalent widths exceeding 0.15 Å in both C IV lines (the A4 sample of SBS but with $\beta_c > 10{,}000$ kms); Figure 4 gives results for the complementary sample of 77 low equivalent width systems. In each of these diagrams the first panel refers to the entire sample of 55 QSOs, the second to a sample with the single quasar 0237−233 eliminated, and the third to a sample in which the additional quasar 0854+191 is also eliminated. Finally, Figure 5 compares our ξ_v estimate for the full sample with estimates for high- and low-redshift subsamples separated at $z = 1.9$. The median redshifts of these two subsamples are 1.61 and 2.30. In all these plots the error bars are the appropriate 1 σ error bars for *unclustered* data derived as discussed above.

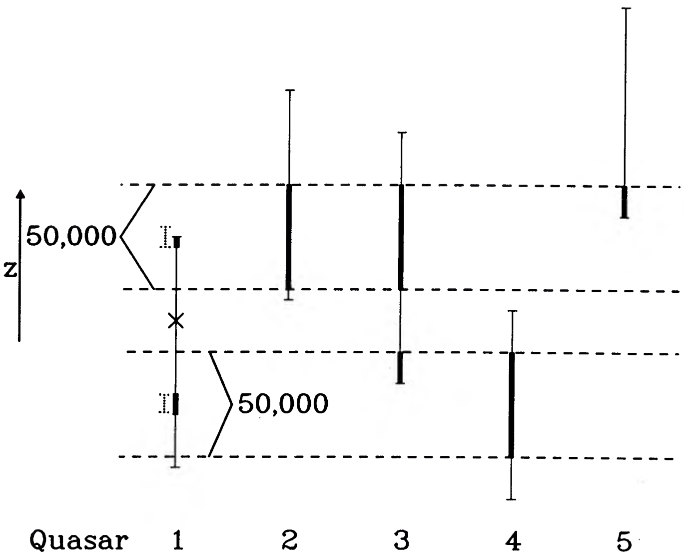

FIG. 1.—Pictorial explanation of the counting algorithm described in the text. Starting from a particular reference system in quasar 1, marked with an (×), we count the number of systems within the small dotted bins that are placed equidistantly in velocity above and below the reference system. Below the reference system the full width of the bin is accessible; however, above, the upper redshift limit for quasar 1 lies within the bin, and thus, the accessible range, as shown by the heavy solid line, is narrower. The expected number of random systems is found by centering over each of the dotted bins a larger interval of 50,000 km s^{-1}; these intervals are shown by dashed lines. For each dashed interval we count the number of systems belonging to the other quasars (e.g., quasars 2–5). We also compute the total path length intersected by each, as represented by heavy solid lines in quasars 2–5. The ratio gives the expected line density for each of the smaller dotted bins. This is multiplied by the accessible range to estimate the number of random systems expected in the bin. We repeat this procedure taking each observed system in turn as the center and accumulating observed expected and random counts in a series of velocity bins. The ratio of the final totals gives our estimate of $1 + \xi_v$.

The first point to note from all these plots is that, for $v > 10{,}000$ km s^{-1}, our estimates of ξ_v are all consistent with zero. A few diagrams appear to show a marginally significant signal in the largest bin. Careful examination of the data shows this to be due to beating between two clusters of systems at opposite ends of the accessible redshift range in the single QSO 0854+191 (see Fig. 6 below). The absence of any systematic trend at large v confirms the generally uniform character of the sample and the lack of any substantial biases. In particular, the estimates of the intervals in each quasar over which C IV lines could have been found must be quite accurate. The fact that $\xi_v \sim 0$ for large v can also be taken as indirect evidence for the identification of the absorbing clouds as intervening objects independent of the QSO.

We clearly detect correlations in the lowest velocity bin ($v < 1000$ km s^{-1}) in all these figures. These correlations are due predominantly to high equivalent width systems, and indeed are detected only at about the 3 σ level in the low equivalent width subsamples. Their amplitude is reduced by a modest factor when 0237−233 and 0854+191 are excluded from the sample. SBS already noted this significant correlation as well as its dependence on equivalent width. If we adopt their bin boundaries, we find an amplitude which differs from theirs by a factor of 1.43. We believe this to reflect the fact that their estimation method implicitly assumes an incorrect estimate of the mean density of absorbing systems. However, as discussed in § II, none of these amplitudes can be translated into standard measures of the strength of spatial clustering without also modeling the internal structure, the kinematics, and the small-scale clustering properties of the absorbers.

On scales beyond 1000 km s^{-1} these problems are probably not important, and our most interesting result is the detection of a significant signal in the range 1000 km s^{-1} < v < 10,000 km s^{-1}. SBS noted that their estimate of ξ_v showed a 2.0 σ excess between 1000 and 10,000 km s^{-1}, and a 2.4 σ deficit between 10,000 and 20,000 km s^{-1}. We confirm this effect, but our analysis shows that above 10,000 km s^{-1} one is reaching the true zero level. This normalization difference is responsible for the different estimates of small-scale correlations referred to in the last paragraph. Figure 2a shows that ξ_v is estimated to be $\sim 0.6 \pm 0.2$ in each of the three bins between 1000 and 10,000 km s^{-1}. In 1000 Monte Carlo trials with unclustered data the largest value in one of these three bins was 0.56, consistent with the estimated 3 σ detection. If this whole range is treated as a single bin we find $\xi_v = 0.63 \pm 0.11$, a 5.4 σ detection. There is again a trend of correlation strength with equivalent width with $\xi_v = 0.6 \pm 0.35$, 1.4 ± 0.36, and 1.6 ± 0.38, for these same three bins in the high equivalent width subsample, or combining them, $\xi_v = 1.19 \pm 0.21$, a 5.6 σ detection. The smaller number of lines gives larger error bars, but the enhancement of the correlation is enough that the significance of the detection is actually slightly increased. For

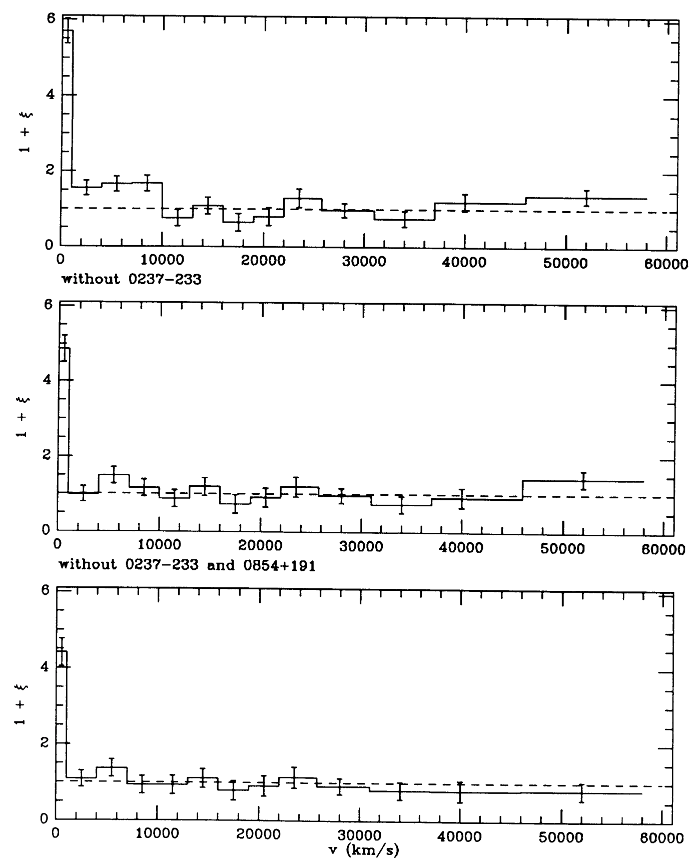

FIG. 2.—Histograms of $1 + \xi_v$ as a function of v; no equivalent width restrictions. In the top panel all 175 systems with $\beta_c > 10{,}000$ km s^{-1} are used. In the second panel the systems in quasar 0237−233 are excluded, and in the bottom panel, those from 0854+191 as well. In all panels a dashed horizontal line is drawn at $\xi_v = 0$.

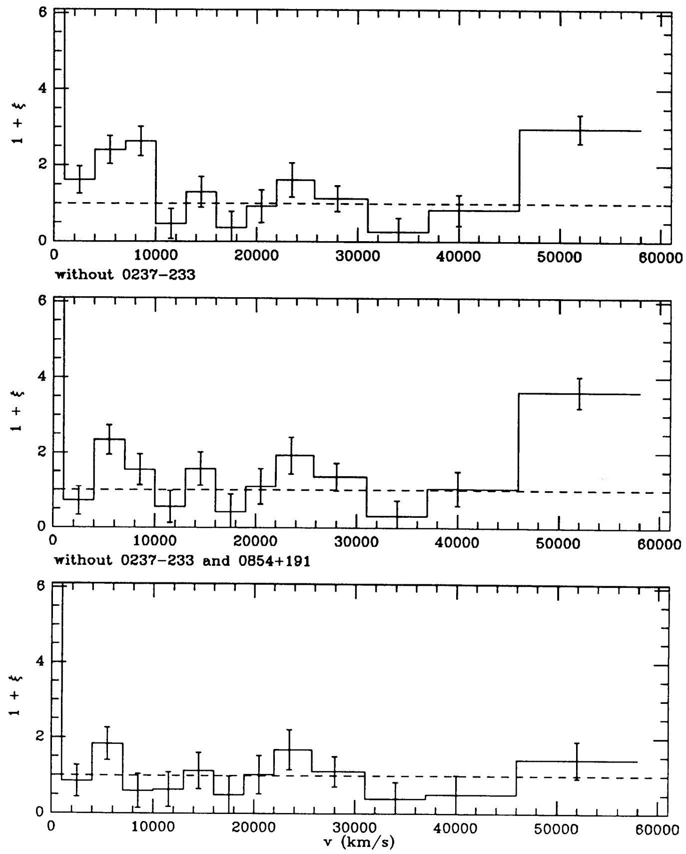

FIG. 3

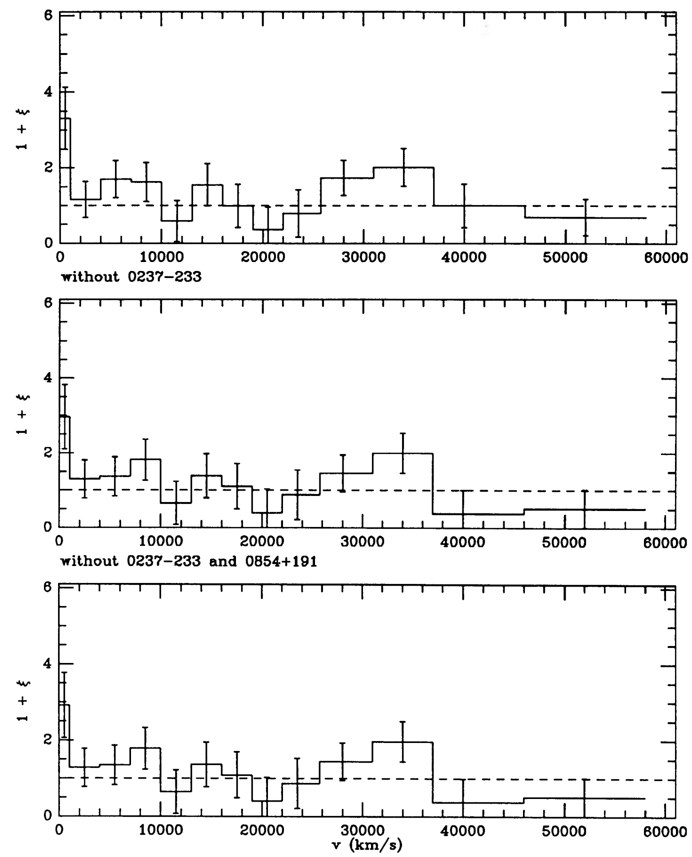

FIG. 4

FIG. 3.—Same as Fig. 2 but counting only the 98 systems with equivalent width exceeding 0.15 Å in both C IV lines.
FIG. 4.—Same as Fig. 3 but for the complementary sample of 77 systems with low equivalent width.

the low equivalent width subsample there is no significant detection of clustering in this range of v.

The amplitude of the signal which we have detected is surprising. For galaxies today $\xi(r)$ is equal to unity at $Hr = 500$ km s^{-1} and is falling as a steep power law. For rich clusters of galaxies the current spatial correlation function falls to zero at 2500 km s^{-1} or less. Even allowing for cosmic deceleration (in a flat universe $v = 10{,}000$ km s^{-1} at $z = 2$ is the comoving scale corresponding to $v = 5774$ km s^{-1} today) the high equivalent width absorption clouds appear significantly more clustered than any currently observed galactic systems. The trend with equivalent width leads one to wonder if this strong correlation might reflect some very large-scale modulation of the ionization structure of the systems, rather than spatial clustering of the clouds themselves.

Our estimate of the significance of this signal is clearly somewhat inflated because the number of independent clumps is smaller than the number of systems. There is no fully model-independent way to estimate the correct size of error bars in plots such as Figures 2–5. However, if we assume that there is no intrinsic clustering on scales exceeding 1000 km s^{-1} we can make some progress.

To be specific, we assume that the distribution consists of uncorrelated clusters of variable richness none of which has a total extent exceeding 100 km s^{-1}. In this situation one can show rigorously that our estimate of ξ_v should vary around zero with an rms scatter bounded above by $(1 + N_c)$ times the

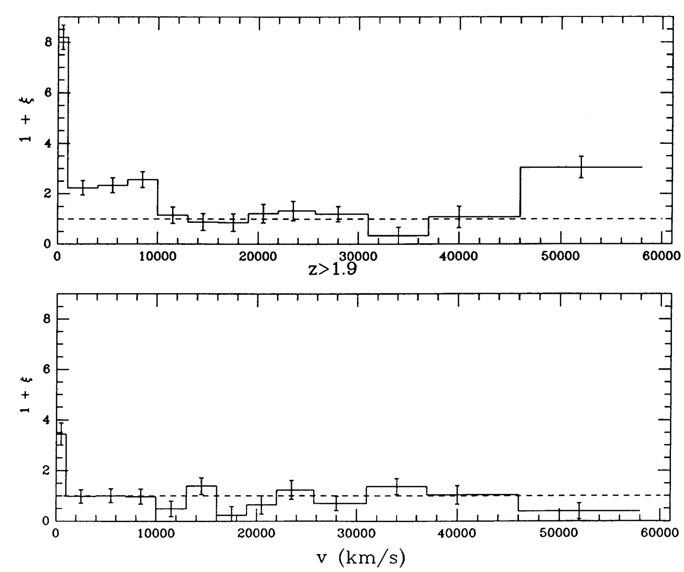

FIG. 5.—Comparison of $1 = \xi_v$ at low and high redshifts. There are no equivalent width restrictions, but $\beta_c > 10{,}000$ km s^{-1}. Top panel is for high redshift ($z > 1.9$), and bottom is for low redshift ($z < 1.9$).

scatter given above for an uncorrelated distribution, where N_c is the average number of absorption systems in excess of random (due to the clustering on < 1000 km s^{-1} scales) along the line of sight to any given system. From the data we find $N_c = 0.50$ for the sample as a whole, and 0.57 for the high equivalent width subsample. We can therefore say that we have detected significant clustering in the 1000 to 10,000 km s^{-1} range at at least the 3.6 σ level for these two samples.

Figure 5 shows that the high clustering amplitude on these scales is due entirely to systems at $z < 1.9$, as is the spurious signal in the largest velocity bin; this can be traced to individual superclusters which happen to lie in the low-redshift range (see below). What may be more significant is a highly significant increase of a factor of 3 in the amplitude of small-scale clustering from the high- to the low-redshift subsample. This is quite striking since their median redshifts ($1 + z = 2.61$ and 3.30) differ by a factor of only 1.26. It is difficult to interpret this rapid growth of apparent clustering because of the complex way it depends on the structure of the clouds and their distribution on very small scales. (See the discussion following eq. [2] above.)

A close examination of the data shows that almost all of the anomalously high correlation between 1000 and 10,000 km s^{-1} is due to a large cluster of systems (itself consisting of two subclusters) in just one QSO, 0237−233. The remainder, as well as the marginal signal in the largest velocity bin, can be attributed to two smaller clusters in 0854+191. In Figure 6 we compare the redshift distribution of absorbers in these two quasars with those of four more typical members of the sample. The extraordinary nature of 0237−233 is very evident from this plot. The considerable influence of these two objects is the reason that we show estimates of ξ_v with one and both of them removed in Figures 2–4. It does not vitiate our estimate of ξ_v for the sample as a whole—the cluster in 0237−233 is a very large system, and shows in itself that clustering extends well beyond 1000 km s^{-1}; however, it does invalidate the assumption made above (the vanishing of two- and three-point functions above 1000 km s^{-1}) in our estimate of sampling fluctuations. As a result we cannot assign a realistic uncertainty to the amplitude of large-scale clustering which we have detected. Notice that the amplitude of small-scale clustering is much less sensitive to the inclusion or otherwise of these two "anomalous" objects.

Although the rich absorption spectrum of 0237−233 is unique in the SBS sample, it is not without precedent. Jacobsen *et al.* (1986) and Sargent and Steidel (1987) have studied an unusual group of southern QSOs within 1° of each other on the sky. The two highest redshift members, which are only 17′ apart, show similarly rich absorption spectra. If one of these is included in our sample in place of 0237−233 (it would not be fair to include both, since the two lines of sight are clearly not statistically independent) we estimate $\xi_v = 0.26 \pm 0.12$ or 0.21 ± 0.12 (for Tol 1037 and Tol 1038, respectively) for the 1000 to 10,000 km s^{-1} range, substantially smaller than our previous estimate but still suggesting significant clustering. The impressive large-scale clustering both in 0237−233 and in Tol 1037/1038 has been noted and discussed previously by Boissé (1987).

In the case of the southern grouping, at least two pieces of evidence suggest that true large-scale spatial correlations are the cause of the signal in ξ_v, rather than, say, high-velocity ejection of multiple absorption clouds from a single active region near the line of sight (see Sargent and Steidel 1987).

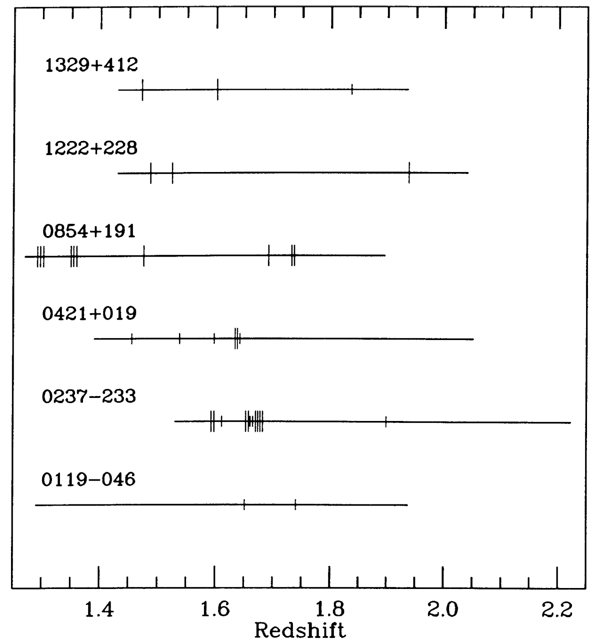

FIG. 6.—The line densities in the unusual quasars 0237−233 and 0854+191 are compared to those found in four typical quasars. Each vertical line represents one C IV system. Long lines are high equivalent width (i.e., >0.15 Å), and short ones signify that at least one line in the system has low equivalent width. (In quasars 0237−233 and 0854+191, the redshifts of some systems were shifted slightly so that they would appear distinct in the plot.)

First there is the coincidence of very rich absorption spectra occurring in two adjacent lines of sight. At least one system lies at the same redshift in both directions (and is also seen in the spectrum of a third, lower redshift QSO), and several other pairs are coincident to within 2000 km s^{-1}. Second, there appears to be an unusual clustering of other QSOs in the same region of sky and in the same redshift range as the highest density of absorption systems. These data add to our confidence that the clustering signal we have detected at large velocity lags in the SBS sample also reflects true spatial correlations in the population of heavy element absorbers. The associated coherence length appears to be at least as large as that currently associated with rich galaxy clusters.

V. DISCUSSION

Since the large-scale clustering signal in the SBS sample is dominated by the "absorption supercluster" in 0237−233, it is clearly of interest to examine this structure in detail. In Figure 6 there are 11 systems over the redshift range $1.5959 < z < 1.6753$, giving the supercluster a line-of-sight depth, L of $\sim 10{,}000$ km s^{-1}. From the sample as a whole we estimate the average number of absorption systems in a 10,000 km s^{-1} interval at this redshift to be 0.57 (or 0.52 if 0237−233 is excluded). Thus the supercluster has an overdensity, δ_{sc}, of ~ 20, for all the systems. It is even greater for high equivalent width systems. Absorption systems with equivalent widths exceeding 15 Å account for eight of the 11 systems in the supercluster, whereas they account for only 98 of the 175 systems in the sample as a whole. This apparently disproportionate representation of high equivalent widths is responsible for much of the enhanced clustering signal in the corresponding estimate of ξ_v (Fig. 3). Finally, we can estimate the fraction of the line of sight occupied by such systems by noting that the total range of velocity surveyed in the lines of sight to all 55 QSOs is 3.14×10^6 km s^{-1}. Since one supercluster with $L = 10^4$ km s^{-1} was found, our best estimate for the one-dimensional filling factor of such systems is $\phi_1 = 1/314$. These numbers allow us to estimate the fraction of absorption systems in superclusters, $F_1 = \delta_{sc}\phi_1$, the redshift-space density of these superclusters, $n_1 = \phi_1/L$, and their typical contribution to the redshift-space correlation function, $\xi_v \sim F_1 \delta_{sc} = \delta_{sc}^2 \phi_1$ on scales of order $L/2$.

Unfortunately, it is not straightforward to translate these numbers into the corresponding three-dimensional properties of the supercluster distribution. As discussed above, we should be able to identify our estimate of ξ_v with the spatial correlation, ξ, on the same scale. In addition, our overdensity estimate should be valid in three dimensions. However, estimates of the abundance and filling factor of the superclusters are sensitive to assumptions about their shape. Let us assume that a supercluster fills a volume fL^3. Thus for near-spherical superclusters we have $f \sim 1$, for "pancakes" with thickness, l, we have $f \sim l/L$, and for filaments of width, l, we have $f \sim (l/L)^2$. We then find that the fraction of absorbing clouds which are members of superclusters is $F_3 \sim \xi/f\delta_{sc} \sim \delta_{sc}\phi_1/f$. Notice that F_3 differs from F_1 by a factor of $1/f$ because we only identify a supercluster in the absorption spectrum if we see it projected along one of its long axes. Notice also that we must require $F_3 < 1$, giving $f > \delta_{sc}\phi_1$. We then obtain the spatial density of superclusters as $n_3 = F_3/\delta_{sc} fL^3 = \phi_1/f^2L^3 = n_1/f^2L^2$, and their three-dimensional filling factor, $\phi_3 = n_3 fL^3 = \phi_1/f$. The lower limit on f implies $n_3 < 1/(\delta_{sc}^2 \phi_1 L^3)$ and $\phi_3 < 1/\delta_{sc}$.

A direct observational test of the geometry of the 0237−233 supercluster can be carried out by examining the absorption line spectra of other nearby QSOs. If the supercluster is roughly spherical, we expect its angular extent to be $\sim 2°$. No spectra for other quasars in this region appear to be available at present, but we hope to obtain such spectra soon.

It may be reasonable to assume that pancakes and filaments form purely by compression along their shorter axes. In this case, $f\delta_{sc} \sim 1$, and all the above three-dimensional quantities can be determined from the observations. We find $F_3 \sim \delta_{sc}^2\phi_1 \sim 1$; almost all absorbing clouds must belong to superclusters. Also, $\phi_3 \sim \phi_1\delta_{sc} \sim 1/15$ and $n_3 \sim L^{-3} = (10{,}000$ km s$^{-1})^{-3}$. With this abundance, a significant number of these superclusters is expected in a volume as large as that surveyed by the largest two-dimensional galaxy catalogs. For example, Groth and Peebles (1977) estimate that the Lick catalog surveys a (current) volume of order $(20{,}000$ km s$^{-1})^3$ and find no evidence for significant *galaxy* correlation amplitudes on scales above 1000 km s^{-1}. In this case the absorbing clouds must be substantially more clustered than galaxies. Thus, in spite of evidence for filamentary superclustering of galaxies (e.g., Oort 1983), the alignment needed to produce our absorption cluster would be exceptionally rare unless superclustering is much more common for absorption clouds than it is for galaxies. On the other hand, if the absorption superclusters are roughly spherical, then $f \sim 1$, their estimated abundance (at $z \sim 2$) drops to $(70{,}000$ km s$^{-1})^{-3}$, and there is a high probability that no such object would be found in the Lick catalog volume. It is then possible that the large-scale clustering amplitude of galaxies has been systematically underestimated, because the observed volume is still too small to be "fair."

Relatively frequent but elongated structures might seem the most natural explanation for our results within current pictures of structure formation. However, the clear discrepancy with current galaxy clustering then suggests that the absorption superclusters cannot have grown purely by gravitational processes. Gravity accelerates everything in the same way. Independent support for this argument comes from the strong dependence of the clustering on C IV equivalent width.

Even if the spatial clustering of the observed absorption systems is real, it may not reflect equally strong clustering of the underlying cloud population. For example, a biasing process may be at work, similar to that invoked by Kaiser (1984) to explain the enhanced clustering of rich galaxy clusters. In this mechanism relatively weak fluctuations in the underlying population are enhanced by some highly nonlinear effect which determines whether any particular cloud reaches the threshold required for detection. The strong dependence of apparent clustering on equivalent width might be taken as evidence in favor of such a bias. However, it is far from obvious how relatively weak variations in cloud abundance could lead to the required large variations in C IV equivalent width.

A more likely explanation might be that C IV equivalent width is spatially modulated by large-scale variations in the ionizing radiation field. An absorption supercluster might then be produced by an unusually powerful QSO or cluster of QSOs acting on an underlying relatively unclustered population of relatively low ionization state. A void in the Lyα forest would presumably occur at the same location; in this model one expects anticorrelation between C IV equivalent width and Lyα line density. This explanation is consistent with the observed prevalence of C IV absorption systems in the neighborhood of QSOs (Foltz *et al.* 1986), and with the presence of QSOs associated with the southern absorption supercluster. Although we find no striking anomalies in the C II/C IV ratios of the absorption systems in the 0237−233 supercluster in comparison with the rest of the sample, there are certainly regimes where variations in ionization parameter could cause the desired effect (Chaffee *et al.* 1986). The sphere of influence required is similar to that found in studies of the "proximity" or "inverse effect" in Lyα forest systems near bright QSOs (Weymann, Carswell, and Smith 1981; Murdoch *et al.* 1986; Bajtlik *et al.* 1988). Although for this supercluster we have not yet identified a candidate QSO which could be producing the ionization, it is possible that it has already burned out and the ionization is a residual light-echo effect.

In conclusion, we have confirmed that the C IV absorbing clouds in the line of sight to quasars are quite strongly clustered at velocity separations less than 1000 km s^{-1}. Unfortunately peculiar velocities of the clouds combine with the one-dimensional nature of the sampling to destroy any possibility of a simple comparison with the amplitude of the clustering of objects observed locally, such as galaxies. On scales of 1000 to 10,000 km s^{-1} clustering persists at a significant amplitude in the SBS sample. This signal is due mainly to absorption systems of high equivalent width and is dominated by the contribution from a single very large "absorption supercluster" in the quasar 0237−233. The implied clustering strength is quite uncertain, but appears larger than that measured for any local population of objects. If real this clustering is probably a result of nongravitational processes.

We are grateful for useful discussions with J. Bechtold, J. Black, F. Chaffee, and C. Foltz. This work was supported by NASA contract NAGW-763 and by NSF Presidential Young Investigator award AST-8352062, and NSF grant AST-8714667.

REFERENCES

Bahcall, N. A., and Soneira, R. M. 1983, *Ap. J.*, **270**, 20.
Bajtlik, S., Duncan, R. C., and Ostriker, J. P. 1988, *Ap. J.*, **327**, 570.
Boissé, P. 1987, in *High Redshift and Primeval Galaxies*, ed. J. Bergeron, D. Kunth, B. Rocca, and J. Tran Thanh Van (Paris: Editions Frontières).
Chaffee, F. H., Foltz, C. B., Bechtold, J., and Weymann, R. J. 1986, *Ap. J.*, **301**, 116.
Davis, M., and Peebles, P. J. E. 1983, *Ap. J.*, **267**, 465.
Dekel, A., Blumenthal, G. R., Primack, J. R., and Olivier, S. 1989, *Ap. J. (Letters)*, **338**, L5.
Foltz, C. B., Weymann, R. J., Peterson, B. M., Sun, L., Malkan, M. A., and Chaffee, F. H. 1986, *Ap. J.*, **307**, 504.
Groth, E. W., and Peebles, P. J. E. 1977, *Ap. J.*, **217**, 385.
Jacobsen, P., Perryman, M. A. C., Ulrich, M. H., Machetto, F., and Di Serego Alighieri, S. 1986, *Ap. J. (Letters)*, **303**, L27.
Kaiser, N. 1984, *Ap. J. (Letters)*, **284**, L9.
Klypin, A. A., and Kopylov, A. I. 1983, *Soviet Astr. Letters*, **9**, 41.
Murdoch, H. S., Hunstead, R. W., Pettini, M., and Blades, J. C. 1986, *Ap. J.*, **309**, 19.
Oort, J. 1983, *Ann. Rev. Astr. Ap.*, **21**, 373.
Salmon, J., and Hogan, C. J. 1986, *M.N.R.A.S.*, **221**, 93.
Sargent, W. L. W., Boksenberg, A., and Steidel, C. C. 1989, *Ap. J. Suppl.*, **68**, 539.
Sargent, W. L. W., and Steidel, C. C. 1987, *Ap. J.*, **322**, 142.
Sutherland, W. 1988, *M.N.R.A.S.*, **234**, 159.
Weymann, R. J., Carswell, R. F., and Smith, M. G. 1981, *Ann. Rev. Astr. Ap.*, **19**, 41.

JULIA HEISLER, CRAIG J. HOGAN, and SIMON D. M. WHITE: Steward Observatory, University of Arizona, Tucson, AZ 85721